ADVANCED FUNCTIONAL MATERIALS
www.afm-journal.de

Ultrathin Iron Oxide Nanowhiskers as Positive Contrast Agents for Magnetic Resonance Imaging

Thomas Macher, John Totenhagen, Jennifer Sherwood, Ying Qin, Demet Gurler, Mark S. Bolding, and Yuping Bao**

In this paper, a highly innovative concept of using ultrathin iron oxide nanowhiskers as a positive (T_1) contrast agent for magnetic resonance imaging (MRI) is demonstrated. Iron oxide nanowhiskers with dimensions of approximately 2 nm × 20 nm are synthesized by heating an iron oleate/oleylamine complex under 150 °C. These nanostructures have very high surface-to-volume ratios, leading to strong paramagnetic signal, a property suitable for T_1 contrast in MRI. The positive contrast enhancement of these nanowhiskers is demonstrated in vitro and in vivo in a rat model. Successful development of this technology has substantial commercial value in biomedical imaging, potentially leading to the advancement of human healthcare technologies.

1. Introduction

Magnetic resonance imaging (MRI) is a powerful, non-invasive imaging tool for diagnosis and post-therapy evaluation.[1] Clinically, contrast agents are routinely applied to enhance the image contrast for better resolution and signal-to-noise ratio.[2,3] Positive contrast agents are mainly paramagnetic gadolinium (Gd) complexes, which shorten the longitudinal relaxation time (T_1) and generate a brighter (T_1-weighted) image. Negative contrast agents, primarily superparamagnetic spherical iron oxide nanoparticles, produce a darker (T_2-weighted) image by shortening the transverse relaxation time (T_2).[4,5] T_1 contrast agents are preferred in the clinical setting as signal enhancement in a lesion after contrast administration is easier to detect than signal attenuation.

Unfortunately, the use of Gd-based contrast agents has raised concerns about nephrogenic systemic fibrosis (NSF) in patients with acute kidney injury, severe renal disease, and liver transplant.[6] The use of Gd- contrast agents was recently reported to lead to brain abnormalities in healthy patients.[7] The potential risks prompted the U.S. Food and Drug Administration (FDA) to issue a black box warning on the use of 5 of 7 Gd-based contrast agents approved in the U.S. All other contrast agents are under observation.[8] Furthermore, Gd-based contrast agents have short blood circulation time by design, which limits their use in targeted and high resolution MRI.[9] Thus, a safer alternative to Gd-based contrast agents is needed.

Iron oxide nanoparticles have limited clinical use as negative (T_2) contrast agents, because these nanoparticles can only passively accumulate in the liver or spleen.[10,11] In addition, signal attenuation after T_2 contrast injection is susceptible to misinterpretation due to other potential sources of signal voids.[12,13] However, iron oxide nanoparticle-based T_2 contrast agents are generally believed to be safe to humans and can be potentially reabsorbed through normal iron metabolic pathways,[14,15] making them a safer alternative than Gd-based contrast agents for patients with renal or hepatic dysfunction. In fact, the clinically available iron oxide nanoparticles, ferumoxytol (trade name: Feraheme), have been used for intravenous iron therapy in adult patients with chronic kidney diseases since 2009.[16] If iron oxide nanoparticles could be developed into T_1 contrast agents, they could potentially provide both improved safety and efficacy, leading to great benefits for human health.

Recently, there is a growing interest in generating positive contrast with iron oxide nanoparticles through the alteration of imaging techniques. Several MR techniques for positive contrast imaging with iron oxide nanoparticles have been explored,[17] such as susceptibility-weighted imaging[18] and phase gradient imaging.[19] Recently, it has been shown that ultrasmall spherical iron oxide nanoparticles (≈3 nm) can generate positive MRI contrast in mice under standard imaging protocols.[20] Therefore, it is feasible to develop T_1 contrast agents for standard clinical scanners by simply adjusting the properties of the nanoparticles.

The potential of using ultrasmall spherical iron oxide nanoparticles (<5 nm) as T_1 contrast agents has been demonstrated by several research groups.[21–24] The rationale of using ultrasmall iron oxide nanospheres as T_1 contrast agents lies in the strong surface effects on their magnetic properties, leading to strong paramagnetic properties. The high surface areas also enhance the water diffusion around the nanoparticles. The

T. Macher, J. Sherwood, Prof. Y. Bao
Chemical and Biological Engineering
Alabama Innovation and
Mentoring of Entrepreneurs
The University of Alabama, Tuscaloosa
AL 35487, USA
E-mail: ybao@eng.ua.edu
Dr. J. Totenhagen, Dr. D. Gurler, Prof. M. S. Bolding
Department of Radiology
The University of Alabama at Birmingham, Birmingham
AL 35233, USA
E-mail: mbolding@uab.edu
Dr. Y. Qin
Alabama Innovation and Mentoring of Entrepreneurs
The University of Alabama
Tuscaloosa, AL 35487, USA

DOI: 10.1002/adfm.201403436

strong paramagnetic property and large surface area for water diffusion make ultrasmall nanospheres good candidates for T_1 MRI contrast agents. For ultrasmall spheres, nanoparticle aggregation is a major concern due to the high surface energy of these particles.[21] In addition, small nanoparticles (<8 nm) generally have fast renal clearance and tend to escape from blood circulation.[25] In addition to ultrasmall spheres, high surface-to-volume (s/v) ratios can also be achieved through shape control (e.g., ultrathin nanowhiskers). The s/v ratio of a 2 nm × 10 nm nanowhisker is close to twice that of a 4 nm spherical nanoparticle.

In this paper, we report a new type of T_1 MRI contrast agent based on ultrathin iron oxide nanowhiskers and demonstrated their feasibility to generate positive enhancement as MRI contrast agents in vitro and in vivo. Specifically, ultrathin iron oxide nanowhiskers (diameter, d < 4 nm) were synthesized using our previously reported selective heating method with a slight modification.[26] These nanowhiskers are about 2 nm × 20 nm in size, exhibiting strong paramagnetic signal due to the large s/v ratios. Subsequently, these nanowhiskers were transferred into aqueous solution using tween-80 as capping molecules via a second layer encapsulation method. The relaxivity of the tween-80 coated nanowhiskers in water was higher than that of the clinically used products. The T_1-weighted image of the nanowhisker water solution showed strong positive contrast enhancement. The T_1-weighted MR images of a Sprague Dawley rat collected on a 3T clinical MRI scanner also showed strong enhancement for both subcutaneous and intraperitoneal injection.

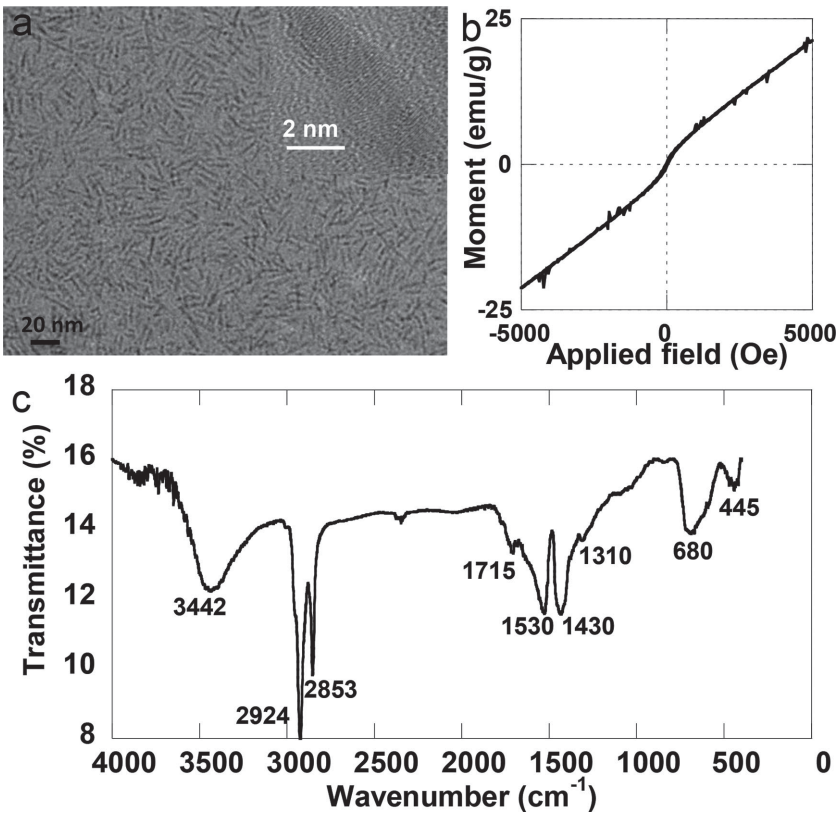

Figure 1. Ultrathin iron oxide nanowhiskers: a) a TEM image, b) a *M–H* curve, and c) a FTIR spectrum.

2. Results and Discussion

The iron oxide nanowhiskers were prepared using our previously published procedure by decomposing the iron (III)-ligand complex at 150 °C with a slight modification.[26] The iron-ligand complex has three coordination ligands, but at this selective temperature, two of the weakly bound ligands decompose first, leaving the third one to direct the formation of the iron oxide nanowhiskers. Here, the modification was the addition of oleylamine as a co-ligand during precursor preparation with oleate to oleylamine ratio of 2 to 1.[27] We have previously shown that the amine functional group had a stronger binding affinity to the iron atoms. The design was that the two oleate ligands will decompose first, and leaving the tightly bound oleylamine as a soft template for nanowhisker formation, which potentially allows for better control of the reaction. Compared to our previous data, this modification allowed for producing iron oxide nanowhiskers with a more uniform diameter and length. **Figure 1**a shows a transmission electron microscopy (TEM) image of the ultrathin iron oxide nanowhiskers (about 2 nm × 20 nm) from a typical reaction. The high resolution TEM image (inset) indicated the crystalline structure and small diameter of these nanostructures. The crystal phase of these nanowhiskers has been previously determined using Raman spectroscopy and X-ray photoelectron spectroscopy to be maghemite phase (γ-Fe_2O_3).[26] The small diameter (≈2 nm) of the nanowhiskers leads to very high s/v ratios.

The magnetic property of a contrast agent indicates whether it is suitable for positive or negative contrast for MRI scans. Generally, T_1 contrast agents are paramagnetic while the T_2 contrast agents are superparamagnetic. The magnetization versus applied field ($M–H$) curve of these nanowhiskers showed a very strong paramagnetic signal without saturation (**Figure 2**b). The strong paramagnetic signal is due to the high s/v ratio and surface iron-ligand complexation. A high percentage of surface iron atoms interacted with the capping molecules through coordination bonds, forming a layer of iron-ligand complexes. The surface layer is mainly paramagnetic, the so-called magnetic "dead layer" on the nanoparticle surfaces, which is commonly observed in small magnetic nanoparticle systems.[28–32] The higher the s/v ratios, the stronger the surface effects on the magnetic properties, as observed in our nanowhisker system.

The FTIR spectra of the nanowhiskers showed the typical absorption bands of 680 and 445 cm^{-1} for spinel structures, where the 680 cm^{-1} bands refers to the Fe–O vibration in the tetrahedral (A)-site and 445 cm^{-1} was assigned to the Fe–O vibration in the octahedral (B)-sites. The carboxylic groups on the nanoparticle surface showed asymmetric and symmetric

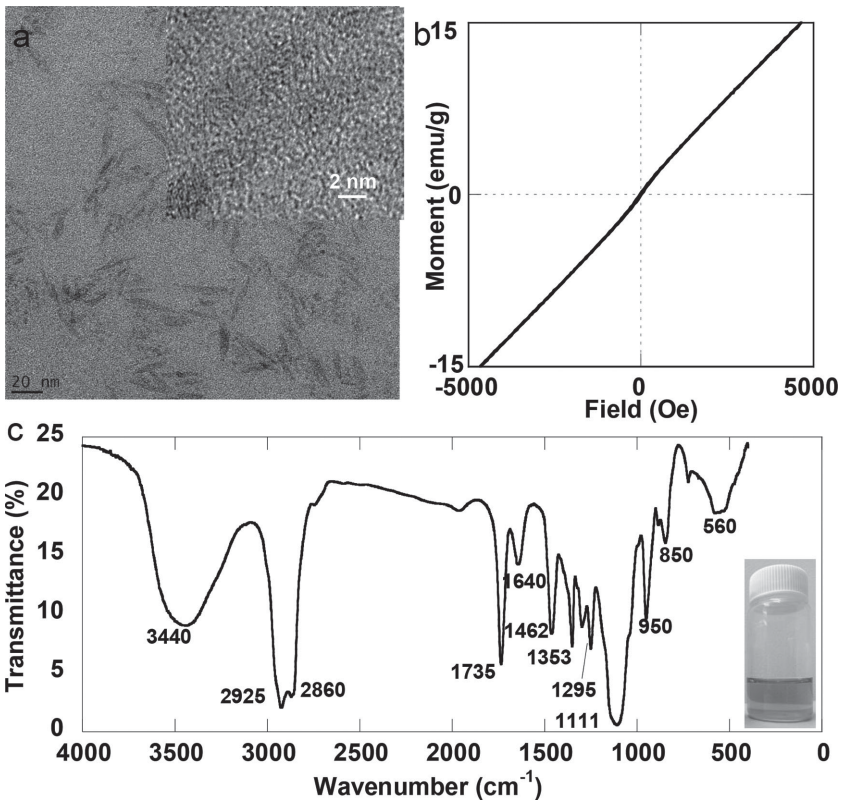

Figure 2. Tween-80 coated ultrathin iron oxide nanowhiskers: a) a TEM image, b) an *M–H* curve, and c) an FTIR spectrum.

vibration of the COO^- groups at 1530 cm^{-1} and 1430 cm^{-1}. The frequency difference of 100 cm^{-1} between the asymmetric and symmetric absorption bands suggested a bidentate binding of carboxylic groups on nanowhiskers surfaces.[33,34] The broad band around 3442 cm^{-1} was assigned to the $–NH_2$ vibration of the oleylamine ligand, an indication of the presence of oleylamine after synthesis. The FTIR spectrum suggests that both oleate and oleylamine are coated on the iron oxide nanowhisker surfaces after the synthesis.

The as-synthesized nanowhiskers are only soluble in organic solvent and they must be transferred into aqueous solution for any biological or biomedical applications. The oleate and oleylamine coated iron oxide nanowhiskers were transferred into aqueous solution using tween-80 as capping molecules through a second layer encapsulation approach.[35] Specifically, polysorbate 80 (tween 80), an amphiphilic biocompatible polymer in water was mixed with nanowhisker organic solution under sonication. The hydrophobic region of tween-80 interacts with the hydrophobic tails of the ligand molecules on the nanowhisker surfaces, leaving the ethylene oxide polymers exposed for water solubility and biocompatibility.

Figure 2 shows a TEM image of tween-80 coated iron oxide nanowhiskers from a typical phase transfer reaction. However, the lattice fringes of the nanowhiskers cannot be clearly resolved from the high resolution TEM image (insert) due to the thick tween-80 coating. After phase transfer, the nanowhiskers were well-dispersed in water, forming clear light brown solution (Figure 2c, insert). The second layer encapsulation did not alter the magnetic properties of the iron oxide nanowhiskers, suggested by the *M–H* curve (Figure 2b). Similar to the organic phase sample, the tween-80 coated nanowhiskers also showed strong paramagnetic signal, but the magnetization decreased because of the increased surface coating thickness from the encapsulation. Because of the further increase in the paramagnetic signal due to surface coatings, the slight magnetic moment observed before tween-80 capping (Figure 1b) was barely detectable in Figure 2b.

The tween-80 encapsulation process was evaluated using FTIR spectroscopy. Several characteristic absorption bands of tween-80 were clearly observed from the FTIR spectrum (Figure 2c). These bands include broad absorption band at 3440 cm^{-1} from –OH stretching and NH_2 stretching, 1735 cm^{-1} band from –C=O stretching of the ester bond, and –C–O–C absorption at 1111 cm^{-1}. Because the tween-80 was wrapped outside of the nanoparticles, the original coating was still present, as indicated by the asymmetric and symmetric $–COO^-$ stretching at 1640 and 1462 cm^{-1}. The iron oxide vibration became one broad band at 560 cm^{-1}. These water soluble nanowhiskers were subsequently used for the relaxivity measurement after dilution.

The effectiveness of a contrast agent is normally evaluated by its relaxivity, given by the equation $1/T_{i\text{sample}} = 1/T_{i\text{sample}} + r_i[M](i = 1,2)$,[3] where, $1/T_{i\text{sample}}$ and $1/T_{i\text{solvent}}$ are the relaxation times of the sample and pure solvent in s^{-1}, $[M]$ is the concentration of the contrast agent in mM, and $r_i(i = 1,2)$ is the relaxivity of the contrast agent. The ratio of the relaxivities, r_2 and r_1 (r_2/r_1) is an indicator of the suitability of a contrast agent for positive (T_1) or negative (T_2) contrast. In general, T_1 contrast agents have a lower r_2/r_1 ratio (e.g., 1–2) while T_2 contrast agents have a larger r_2/r_1 ratio (>10).[36] The relaxivity of the iron oxide nanowhiskers were measured on a Bruker minispec mq-60 60 MHz NMR Relaxometer (1.4 T). The relaxation curves of iron oxide nanowhiskers water solution are shown in **Figure 3**a and b. The T_1 relaxation rate was recorded using the Saturation Recovery Pulse Sequence (t_1_sr_mb) and the T_2 relaxation rate was recorded using the Carr-Purcell-Meiboom-Gill (CPMG) spin echo method (t_2_cp_mb). The relaxation rate of pure water was used as background. The iron concentration was determined using inductively coupled plasma mass spectrometry (ICP-MS). Using the relaxivity equation, the r_1 and r_2 relaxivities of the iron oxide nanowhiskers were calculated to be 6.13 s^{-1} mM^{-1} and 11.15 s^{-1} mM^{-1}. The r_2/r_1 ratio of 1.83 suggested the potential of the iron oxide nnowhiskers serving as T_1 MRI contrast agents. The absolute relaxivity, r_1, of these nanostructures was higher than the clinically used Magnevist (Gd-DTPA, 4.2 mM^{-1} s^{-1}), also suggest their potential efficiency.

To confirm their suitability as MRI contrast agents, in vitro T_1-weighted images of nanowhiskers in water were collected on

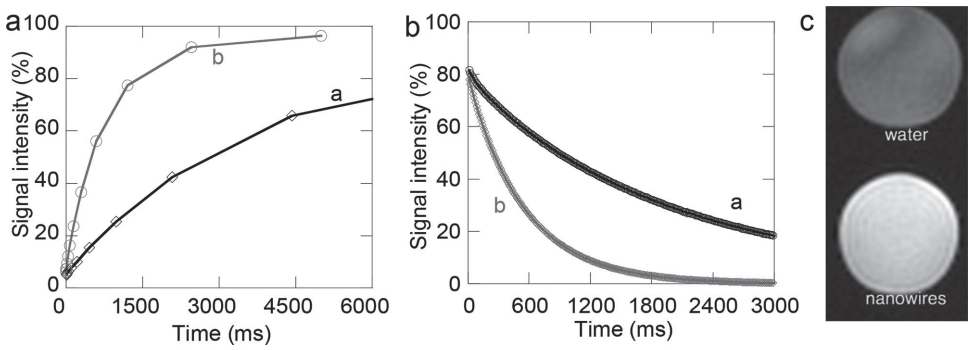

Figure 3. Tween-80 coated nanowhiskers in water: a) T_1 relaxation curve (a-water control, b-nanowhisker water solution), b) T_1 relaxation curve (a-water control, b- nanowhisker water solution), and c) T_1-weighted maps of water and nanowhisker water solution.

a Siemens Allegra 3T clinical MRI using a standard T_1-weighted spin echo sequence (t1_se_sag). Sequence parameters were: TR 600 ms, TE 35 ms, flip angle 60°, acquisition matrix 256^2, FOV 256^2 mm, slice thickness 5 mm. The phantom images of the iron oxide nanowhiskers solution and water background are shown in Figure 3c. The obtained images showed very high contrast with a TR of 600 ms. Thus, it was found that the iron oxide nanowhiskers have a strong T_1-shortening capability as MRI contrast agents.

Figure 4a–c shows T_1-weighted MR images of a Sprague Dawley rat (412 g) collected on a 3T clinical MRI scanner (Philips Achieva). The animals were anesthetized with isoflurane (1–2%) and imaged with an 8 channel head coil. Nanowhisker contrast agent (0.17 mg Fe /mL) was injected intraperitoneally (IP; 6 mL) and subcutaneously (1 mL). T_1-weighted MR images of the animals were recorded pre injection and 1 min post injection. Sequence parameters were TR 600 ms, TE 10 ms, acquisition matrix 512^2, FOV 230^2 mm, slice thickness 4 mm. In Figure 1b, the abdominal region of the IP injected animal shows brightening compared with the pre injection image in Figure 1a, suggesting the strong positive contrast enhancement of iron oxide nanowhiskers. The bleb from the subcutaneous injection (circle) clearly shows T_1 enhancement due to the contrast agent (Figure 4c). There is an apparent difference in enhancement at the two injection sites. Further investigations are required to determine the cause of this difference. This difference may be due to a difference in final dilutions of the contrast agent or it might be due to interactions of the nanowhiskers with the differing physiological conditions in the two compartments. Both of these studies indicated the feasibility of generating positive contrast enhancement in vivo using ultrathin iron oxide nanowhiskers under standard MRI settings.

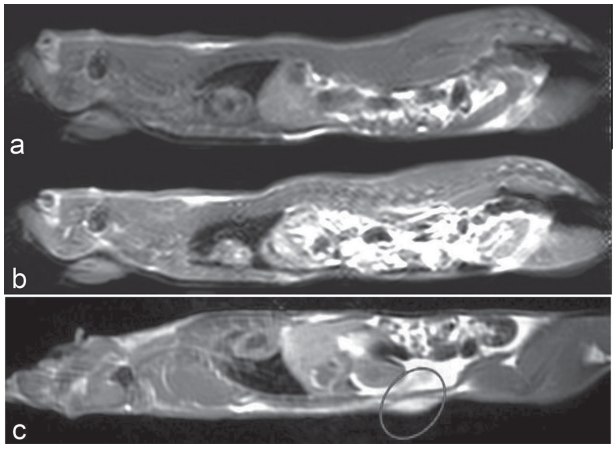

Figure 4. T_1-weighted in vivo images of nanowhisker contrast agent at 3T: a) Pre injection image without nanowhiskers, b) post injection image showing positive enhancement of the abdominal region. 6 mL of contrast agent was injected IP, and c) subcutaneous injection of 1 mL of nanowhiskers at 2 mg/mL concentration. The circle indicates the bleb at the site of injection.

3. Conclusion

In summary, we have successfully demonstrated the innovative concept of using ultrathin iron oxide nanowhiskers as T_1 MRI contrast agents. The extremely high s/v ratio of the nanowhiskers led to strong paramagnetic signal, making them more suitable as T_1 contrast agents. The high r_1 relaxivity of these nanostructures and the lower r_2/r_1 ratio also indicated their potential as effective T_1 MRI contrast agents. Most impressively, the positive enhancement in vivo on rats was observed from both subcutaneous and intraperitoneal injections of the nanowhiskers. Further studies, such as blood circulation time and biodistribution, need to be performed to fully evaluate the potential of these nanowhiskers. The successful development of this product will not only fulfill the need of patients with special conditions during an MRI scan, but also greatly benefit healthy patients who need MRI scans, potentially leading to the advancement of human health.

Supporting Information

Supporting Information is available from the Wiley Online Library or from the author. Experimental details: this material is available free of charge via the Internet at http://pubs.acs.org.

Acknowledgements

This work was supported in part by NSF-DMR 0907204 and DMR1149931. The authors acknowledge the UA Central Analytical

Facility (CAF) and the Biological Science Department for the use of TEM and Marie Warren for assistance with the animal imaging experiments.

Received: October 1, 2014
Revised: October 30, 2014
Published online: December 1, 2014

[1] E. Terreno, D. D. Castelli, A. Viale, S. Aime, *Chem. Rev.* **2010**, *110*, 3019–3042.
[2] E. A. Waters, S. A. Wickline, *Basic Res. Cardiol.* **2008**, *103*, 114–121.
[3] G. J. Strijkers, W. J. M. Mulder, G. A. F. van Tilborg, K. Nicolay, *Anti-cancer Agents Med. Chem.* **2007**, *7*, 291–305.
[4] FDA approval for Feridex iv liver contrast agent. Drug News Perspectives **1996**, *9*, 422–422.
[5] P. Reimer, T. Balzer, *Eur. Radiol.* **2003**, *13*, 1266–1276.
[6] K. M. Hasebroock, N. J. Serkova, *Expert Opin. Drug Metab. Toxicol.* **2009**, *5*, 403–416.
[7] T. Kanda, K. Ishii, H. Kawaguchi, K. Kitajima, D. Takenaka, *Radiol.* **2014**, *270*, 834–842.
[8] http://www.fda.gov/Drugs/DrugSafety/ucm223966.htm (accessed: June 2011).
[9] N. Lee, T. Hyeon, *Chem. Soc. Rev.* **2012**, *41*, 2575–2589.
[10] B. Hamm, T. Staks, M. Tapuitz, R. Maibauer, A. Speidel, A. Huppertz, T. Frenzel, R. Lawaczeck, K. J. Wolf, L. Lange, *J. Magn. Res. Imag.* **1994**, *4*, 659–668.
[11] D. C. Baiu, C. Brazel, Y. Bao, M. Otto, *Curr. Pharm. Des.* **2013**, *19*, 6606–6621.
[12] J. C. Brisset, M. Sigovan, F. Chauveau, A. Riou, E. Devillard, V. Desestret, M. Touret, S. Nataf, J. Honnorat, E. Canet–Soulas, N. Nighoghossian, Y. Berthezene, M. Wiart, *Mol. Imag. Biol.* **2011**, *13*, 672–678.
[13] Y. Okuhata, *Adv. Drug Deliv. Rev.* **1999**, *37*, 121–137.
[14] R. Weissleder, D. D. Stark, B. L. Engelstad, B. R. Bacon, C. C. Compton, D. L. White, P. Jacobs, J. Lewis, *Am. J. Roentgenol.* **1989**, *152*, 167–173.
[15] D. D. Stark, R. Weissleder, G. Elizondo, P. F. Hahn, S. Saini, L. E. Todd, J. Wittenberg, J. T. Ferrucci, *Radiol.* **1988**, *168*, 297–301.
[16] M. Lu, M. H. Cohen, D. Rieves, R. Pazdur, *Am. J. Hematol.* **2010**, *85*, 315–319.
[17] C. H. Lin, S. H. Cai, J. H. Feng, *J. Nanomater.* **2012**, *734842*, 1–9.
[18] F. Eibofner, G. Steidle, R. Kehlbach, R. Bantleon, F. Schick, *Magn. Reson. Med.* **2010**, *64*, 1027–1038.
[19] H. T. Zhu, K. Demachi, M. Sekino, *Magn. Reson. Imag.* **2011**, *29*, 891–898.
[20] M. Park, N. Lee, S. H. Choi, K. An, S. H. Yu, J. H. Kim, S. H. Kwon, D. Kim, H. Kim, S. I. Baek, T. Y. Ahn, O. K. Park, J. S. Son, Y. E. Sung, Y. W. Kim, Z. W. Wang, N. Pinna, T. Hyeon, *Chem. Mater.* **2011**, *23*, 3318–3324.
[21] U. I. Tromsdorf, O. T. Bruns, S. C. Salmen, U. Beisiegel, H. Weller, *Nano Lett.* **2009**, *9*, 4434–4440.
[22] J. Y. Park, E. S. Choi, M. J. Baek, G. H. Lee, S. Woo, Y. Chang, *Eur. J. Inorg. Chem.* **2009**, 2477–2481.
[23] E. Taboada, E. Rodriguez, A. Roig, J. Oro, A. Roch, R. N. Muller, *Langmuir* **2007**, *23*, 4583–4588.
[24] Z. Li, P. W. Yi, Q. Sun, H. Lei, H. L. Zhao, Z. H. Zhu, S. C. Smith, M. B. Lan, G. Q. Lu, *Adv. Funct. Mater.* **2012**, *22*, 2387–2393.
[25] M. Longmire, P. L. Choyke, H. Kobayashi, *Nanomed.* **2008**, *3*, 703–717.
[26] S. Palchoudhury, W. An, Y. L. Xu, Y. Qin, Z. T. Zhang, N. Chopra, R. A. Holler, C. H. Turner, Y. P. Bao, *Nano Lett.* **2011**, *11*, 1141–1146.
[27] S. Palchoudhury, Y. L. Xu, W. An, C. H. Turner, Y. P. Bao, *J. Appl. Phys.* **2010**, *107*, 09b311–314.
[28] P. Guardia, B. Batlle-Brugal, A. G. Roca, O. Iglesias, M. P. Morales, C. J. Serna, A. Labarta, X. Batlle, *J. Magn. Magn. Mater.* **2007**, *316*, E756–E759.
[29] H. Kachkachi, A. Ezzir, M. Nogues, E. Tronc, *Eur. Phys. J. B* **2000**, *14*, 681–689.
[30] Y. Koseoglu, H. Kavas, B. Aktas, *Phys. Stat. Sol. Appl. Mater. Sci.* **2006**, *203*, 1595–1601.
[31] A. Millan, A. Urtizberea, N. J. O. Silva, F. Palacio, V. S. Amaral, E. Snoeck, V. Serin, *J. Magn. Magn. Mater.* **2007**, *312*, L5–L9.
[32] Y. Koseoglu, H. Kavas, *J. Nanosci. Nanotechnol.* **2008**, *8*, 584–590.
[33] K. Nakamoto, *Infred and Raman Spectra of Inorganic and Coordination Compounds*, 4th ed., John Wiley & Sons, New York **1986**.
[34] H. B. Abrahamson, H. C. Lukaski, *J. Inorg. Biochem.* **1994**, *54*, 115–130.
[35] A. Prakash, H. G. Zhu, C. J. Jones, D. N. Benoit, A. Z. Ellsworth, E. L. Bryant, V. L. Colvin, *ACS Nano* **2009**, *3*, 2139–2146.
[36] U. I. Tromsdorf, N. C. Bigall, M. G. Kaul, O. T. Bruns, M. S. Nikolic, B. Mollwitz, R. A. Sperling, R. Reimer, H. Hohenberg, W. J. Parak, S. Forster, U. Beisiegel, G. Adam, H. Weller, *Nano Lett.* **2007**, *7*, 2422–2427.